



Effect of Facial-seal Leaks on Protection Provided by Half-mask Respirators

William C. Hinds & Peter Bellin

To cite this article: William C. Hinds & Peter Bellin (1988) Effect of Facial-seal Leaks on Protection Provided by Half-mask Respirators, Applied Industrial Hygiene, 3:5, 158-164, DOI: [10.1080/08828032.1988.10388550](https://doi.org/10.1080/08828032.1988.10388550)

To link to this article: <https://doi.org/10.1080/08828032.1988.10388550>



Published online: 25 Feb 2011.



Submit your article to this journal [↗](#)



Article views: 38



View related articles [↗](#)



Citing articles: 15 View citing articles [↗](#)

Effect of Facial-seal Leaks on Protection Provided by Half-mask Respirators

William C. Hinds and Peter Bellin

University of California Southern Occupational Health Center, UCLA School of Public Health, Los Angeles, California 90024

Applications are presented of a computer model that gives the performance (overall protection factor including filter penetration and facial-seal leakage) of half-mask respirators for protection against aerosols. Input variables for the model are type of filter used, work rate of the wearer, QNFT-measured fit factor, and size distribution of the exposure aerosol. Based on the model, measurement errors due to loss of particles in leaks during qualitative fit testing (QNFT) measurements with current equipment are estimated to be less than 5 percent, but the change from high efficiency test filters to regular dust, fume, and mist (DFM) filters in use can reduce protection significantly. Overall protection factors are predicted for 33 industrial exposures based on assumed QNFT fit factors of 20 and 50. In these examples, DFM respirators with a QNFT fit factor of 50 have predicted protection factors from 21 to 2900, depending on aerosol size distribution. Overall protection factors for disposable and DFM filter respirators having a given facial-seal leak are presented graphically for a wide range of aerosol size distributions and two work rates. Also given is a contour chart showing the QNFT fit factor required to achieve an overall protection factor of 20 or 50 for a wide range of aerosol size distributions. For an unknown aerosol size distribution and average respirator performance (half-mask with DFM filters), a QNFT fit factor of 15 or more is required to ensure an overall protection factor of at least 10. Hinds, W. C.; Bellin, P.: *Effect of Facial-seal Leaks on Protection Provided by Half-mask Respirators*. *Appl. Ind. Hyg.* 3:158-164; 1988.

Introduction

Two mechanisms can diminish the respiratory protection provided by a half-mask respirator: 1) penetration through the filter or cartridge and 2) facial-seal leakage. In most cases where respirators are used for protection against gases or vapors, it is reasonable to neglect the cartridge penetration, in the absence of breakthrough, if the respirator is properly selected and used. On the other hand, for respirators used to protect against aerosols, both paths represent potentially important avenues of exposure and both are strongly particle size dependent;⁽¹⁻²⁾ that is, the extent of exposure depends on the size of the aerosol

particles present. Furthermore, the particle size dependence is controlled by the instantaneous flow rate through the respirator, so penetration and leakage depend on the work rate of the wearer and are constantly changing during each breathing cycle.

In normal use, the mass concentration and particle size distribution inside the respirator, that which the wearer is exposed to, differ greatly from that outside the respirator where these quantities are usually measured. This makes estimation of a respirator wearer's exposure in use and verification of adequate protection a difficult task.

Despite these complexities, there are many situations for which it is desirable to evaluate the actual exposure of a respirator wearer, that is the concentration or amount of contaminant he or she is breathing. Examples of such situations include the following: 1) good industrial hygiene practice where it is always desirable to know the actual exposure experienced by each worker (the "evaluation" component of "recognition, evaluation, and control"), 2) epidemiological studies where accurate exposure assessment is needed to establish associations between exposure and the occurrence of symptoms or disease, 3) liability protection, 4) industrial hygiene evaluation as follow-up to observed occurrence of disease or symptoms, and 5) design and development of improved respirators by respirator manufacturers.

Overall respirator performance for protection against aerosols depends on 1) filter penetration, 2) facial-seal leakage (air flow rate), and 3) particle penetration through facial-seal leaks (the relative ability of different size particles to pass through leaks). All three depend on breathing rate which in turn depends on the work rate of the wearer, and the first and third depend on the particle size distribution to which he or she is exposed. In this paper, work rate is expressed in kg-m/min. A work rate of 0 kg-m/min corresponds to workers standing still or seated; 622 kg-m/min (approximately 430 kcal/hr) represents moderate to hard work that can be sustained for a period of several hours. Inhaled volumes are 14.2 and 37.3 L each minute for 0 and 622 kg-m/min, respectively.⁽³⁾ Work rate can exceed 622 kg-m/min for brief periods such as emergency situations or ladder climbing.

To put into perspective the role that the three factors identified above play in the performance of a respirator, the predictive

model for respirator performance described below was used to estimate the range of penetration that results from the usual and appropriate range of applications of average dust, fume, and mist (DFM) half-mask cartridge respirators. Filter penetration can range from less than 0.03 percent, for a coarse dust like coal mine dust when the respirator is used at a low work rate, to 2.4 percent for welding fume at a high work rate. This 80-fold difference corresponds to protection factors ranging from 42 to 3300.

As discussed by Hinds and Kraske in a previous paper,⁽¹⁾ the proportion of the inhaled air that goes through a facial seal leak varies with the breathing rate. Thus, the same respirator with the same fit might have a workplace protection factor (reciprocal of facial seal leakage plus filter penetration) that changes by a factor of three as the workrate of the wearer changes from 0 to 622 kg-m/min.

Finally, aerosol particles less than 2 μm in aerodynamic diameter pass through leaks nearly undiminished, whereas particles $> 5 \mu\text{m}$ are significantly reduced in number as they pass through leaks. As a result of this differential particle leak penetration, the workplace protection factor for a half-mask respirator with a perfect filter may vary by a factor of three for the usual range of particle size distributions.

Assigned protection factors, while providing a convenient measure of minimum protection, do not take into account the unique penetration characteristics of aerosols outlined above; consequently, they provide only a crude indication of the actual exposure of the wearer. One may be tempted to use the National Institute for Occupational Safety and Health/Mine Safety and Health Administration (NIOSH/MSHA) certification tests, such as the silica dust or lead fume tests, as a basis for estimating filter performance. These tests are conducted for limited and specific size distributions, and, although they require high average efficiency ($> 99\%$), the conditions of the test involve heavy loading which enhances aerosol capture efficiency. Thus, one can not assume such high efficiency under more representative light loading conditions.

Previous Work

Previous attempts to model the performance of respirators have been described by Silver *et al.*⁽⁴⁾ using an electrical analog, and by Campbell⁽⁵⁾ and Williams⁽⁶⁾ using a steady flow model. Neither type takes into account the variation in performance associated with aerosol particle size. The respirator performance model for aerosols described by Hinds and Bellin⁽²⁾ is the most complete. It takes into account all the factors outlined above and predicts the overall performance of a respirator and filter combination having a known or measured leakage for any work rate and aerosol size distribution.

The Hinds and Bellin model is based on detailed experimental measurements of filter penetration as a function of particle size (aerodynamic diameter) and flow rate and on experimental measurements of facial-seal leakage as a function of particle size (aerodynamic diameter), leak size, and pressure drop (difference in pressure between the inside and outside of the mask). Some 1600 penetration measurements were made for each filter or leak tested. These data are reduced to form a data base matrix of 98 penetration values (7 flow rates and 14 particle sizes) for each filter or leak tested. Performance data for a specific filter and average data for facial-seal leaks are combined in the correct proportion in a Lotus 1-2-3 spreadsheet and integrated over the breathing (inhalation) cycle associated with six work rates, seden-

tary to 830 kg-m/min. The result is the combined penetration (leakage plus filter penetration) for 14 particle sizes, 0.14 to 11 μm , for each work rate. These data are used in a BASIC program that integrates penetration on a mass or count basis for a given work rate over a lognormal particle size distribution with a specified mass median aerodynamic diameter (MMAD) and geometric standard deviation (GSD).

This paper presents some applications of this model to the prediction of overall respirator performance for a range of conditions likely to be found in industry.

Applications

QNFT Measurement Errors

One application of the model is to evaluate certain errors associated with quantitative fit testing (QNFT). Two types of errors are considered here: 1) the measurement error due to the attenuation of larger test aerosol particles as they traverse facial-seal leaks and 2) the difference in overall performance that results from using high efficiency filters for testing and standard (DFM) filters in the workplace. The second has two counteracting effects: pressure drop may be reduced with the standard filter causing a decrease in leakage, and small particles can penetrate the standard DFM filter in significantly greater quantities compared to the high efficiency filter.

The sodium chloride (NaCl) fit testing apparatus measures the mass concentration of NaCl aerosol outside and inside the mask while it is being worn. The direct-reading analytical method uses flame photometry to measure the intensity of sodium emission as the aerosol passes through a natural gas flame. The output signal is proportional to the number of sodium atoms present and thus measures relative aerosol mass directly. The reported size distribution for the NaCl test aerosol is a MMAD of 0.48 to 0.72 μm and a GSD of 1.8 to 2.0.⁽⁷⁻⁹⁾

Penetration measurements made with a corn oil (or DOP) fit testing apparatus are more difficult to interpret because forward light scattering (scattering angle 13 to 43 degrees) is used to estimate aerosol concentrations outside and inside the mask. Forward light scattering is a strong function of particle size, so that the changes in test aerosol size distribution that occur as a result of preferential capture in filters or leaks can modify the signal to mass ratio. The reported size distribution for the corn oil test aerosol is a count median diameter (CMD) of 0.25 μm and a GSD of 1.53.⁽¹⁰⁾

The model was used to estimate the error in measured QNFT fit factor associated with the loss of larger particles in leaks. To accomplish this, filter penetration was assumed to be zero, and an average leak performance curve was used with published test aerosol size distributions. Numerical Simpson's rule integration over the size distribution was done to get the mass penetration, that is, the mass of particles traversing the leak divided by the mass of particles originally in the air that passes through the leak.

For the NaCl aerosol at a work rate of 0 kg-m/min, 96 percent of the aerosol mass will penetrate a facial-seal leak; at a 622 kg-m/min work rate, penetration is slightly lower at 95 percent. A similar analysis for corn oil was conducted, but here one must take into account the differences in light scattering properties of the inside and outside aerosols. For this estimate, the relative light scattering over a 13 to 43 degree range of scattering angles for corn oil droplets was computed using a FORTRAN subroutine⁽¹¹⁾ and integrated over the inside and outside size distributions to determine their relative signals. Results suggest

that over the normal range of work rates, a corn oil QNFT measurement will indicate 97 percent of the potential mass leakage. Although there are significant differences in light scattering over the corn oil particle size range, leak penetration is not size dependent in this size range, and, consequently, the systematic measurement error is slight.

These calculations were also made using the recommended particle size limits for QNFT test aerosols given in ANSI Z88.2-1980, specifically a MMAD of 0.5 to 0.7 μm and a GSD of 2.0 to 2.4.⁽¹²⁾ For these size distribution limits, the NaCl apparatus will indicate 93 to 96 percent and the corn oil apparatus 77 to 95 percent of the potential facial-seal leakage. The difference between the NaCl and corn oil results is due to the light scattering

effect described above.

In the above analysis, penetration through high efficiency dust, fume, mist, and radionuclides (DFMR) filters was assumed to be zero. Although high efficiency cartridge filters have much lower penetration than DFM cartridge filters, great variation existed among the four brands tested. At a steady flow of 10 liters per minute (lpm), average submicrometer penetration ranged from 0.0008 to 1.41 percent; at 100 lpm, penetration ranged from 0.005 to 0.75 percent. Clearly, filter penetration can be neglected for the most efficient filter but not for the least efficient. Indeed, QNFT testing using the least efficient of the four DFMR filters tested would not be able to measure fit factors greater than about 100.

TABLE I. Aerosol Size Distributions for Various Industrial Operations and Predicted Overall Protection Factors for QNFT Fit Factor of 20 and 50

Operation	MMAD, μm	GSD	Predicted PF ^a		Ref.
			QNFT FF = 20	QNFT FF = 50	
Mining					
Open pit, general environment (ns) ^{b,c}	2.5	4.7	36	67	13
Open pit, in cab (2)	1.1	2.4	26	48	13
Coal mine, continuous miner (27)	4.6	2.5	56	132	14
Coal mine, continuous miner (8)	15.0	2.9	158	386	15
Coal mine, continuous miner (50) ^c	17.0	3.1	172	419	16
Coal mine, other operations (80) ^c	11.5	2.8	122	298	16
Oil Shale mine (26)	2.8	3.5	39	79	17
Smelting and Foundry					
Lead smelter, sintering (7) ^c	11.0	2.4	130	322	18
Lead smelter, furnace (8) ^c	3.3	15.7	47	79	18
Brass foundry, pouring (4) ^c	2.1	10.3	38	64	18
Brass foundry, grinding (3) ^c	7.2	12.9	52	90	18
Iron foundry, general environment (1)	2.8	5.1	38	70	19
Iron foundry, general environment (4)	16.8	4.4	127	290	20
Be-Cu foundry, furnace (16)	5.0	2.4	59	142	21
Nuclear fuel fabrication (66)	2.1	1.6	35	85	22
Non-mineral Dust					
Bakery (6)	12.1	4.2	99	222	23
Cotton gin (5) ^{c,d}	47.1	2.7	1150	2860	24
Cotton mill (10)	7.6	4.0	72	158	25
Swine confinement building (21) ^c	9.6	4.0	83	186	26
Woodworking, machining, sanding					
fine mode (6)	1.3	2.7	27	51	27
coarse mode (6)	33.1	2.6	687	1710	27
Wood model shop (9)	7.2	1.4	92	229	28
Metal Fume					
SMA (stick) Welding (ns) ^p	0.38	1.8	17	25	29
MIG Welding (ns) ^p	0.48	2.3	19	29	29
Lead fume (O ₂ -Nat. gas) (5)	0.37	2.1	17	26	30
Mist and Spray					
Pressroom, ink mist (10)	27.4	4.30	226	529	31
Spray painting, lacquer (ns)	6.4	3.4	68	152	32
Spray painting, enamel (ns)	5.7	2.0	67	165	32
Aerosol spray products (6) ^c	6.4	1.8	76	189	33
Other					
Forging (ns) ^c	5.5	2.0	65	161	34
Refinery, fluid catalytic cracker (4) ^p	6.2	2.4	70	171	35
Cigarette smoke (diluted) (5)	0.4	1.4	17	25	36
Pistol Range (2)	2.6	3.8	37	73	37
Diesel exhaust (age = 5-600 s) (5)	0.12	1.4	16	21	38

^aPredicted protection factors are based on the following assumptions: measured QNFT fit factors are 20 or 50, QNFT test conducted at a work rate of 0 kg-m/min with perfect DFMR filters having average resistance, respirator is properly used at a work rate of 415 kg-m/min with average DFM filters.

^bNumber in parenthesis following the operation name is the number of size distributions on which the data in the table are based; ns = number of size distributions not specified.

^cAverage values for MMAD and GSD used (median values used for all others).

^dMass distribution parameters calculated from count distribution data.

A comparison of the resistance of DFM and DFMR filters for four brands reveals substantial differences. The ratio of DFM filter resistance to DFMR filter resistance ranged from 0.29 to 1.49 for the same brand. At a work rate of 0 kg-m/min, these differences would typically cause facial-seal leakage to change by -61 percent to +35 percent as one switches from fit testing with DFMR filters to use with DFM filters.

Taking all of the above into account, one can conclude that, using current equipment, systematic measurement errors of facial-seal leakage will usually be less than 5 percent, within experimental accuracy for this type of measurement. However, as explained previously, the use of QNFT tests to estimate field protection factors may be significantly in error for three reasons: 1) the breathing rate in actual use may differ from the test conditions, 2) the use of a less efficient filter will allow greater filter penetration, and 3) the use of a filter with less resistance will decrease leakage. As a consequence of these effects, it is necessary to use a model such as the one described here or field measurements to estimate workplace protection factors realistically from QNFT fit factors. The use of the model described here requires the additional assumptions that the fit measured by QNFT is representative of the fit achieved in use and that there are no sampling errors during QNFT.

Predicting Respirator Performance

A comparison between measured fit factors and the predicted performance in use for half-mask respirators in selected industrial aerosol exposures is given in Table I. The size distributions given in Table I represent a compilation of published studies giving aerosol size distributions in terms of either MMAD and GSD or data for which these values could be easily estimated. Some data were excluded because they did not appear to have a lognormal distribution. For those studies reporting multiple size distributions, the median of the distribution parameters was used to provide a representative single value for the MMAD and GSD. Conditions for predicted protection factors are zero percent

penetration of test aerosol through high efficiency test filters having average resistance and a 0 kg-m/min average work rate during QNFT fit testing. Arbitrarily selected QNFT fit factors of 20 and 50 as measured by corn oil QNFT were used. It is further assumed that in use the worker has the same fit as during the QNFT and that DFM filters having average performance characteristics are used at a work rate of 415 kg-m/min. The work rate of 415 kg-m/min was chosen because it is a moderate work rate typical of many industrial situations.

One can conclude from Table I that for most of the exposure conditions given, an accurate and representative QNFT test will provide a conservative estimate of in-use performance. In extreme cases (large particle size distributions), performance in use is underestimated by the QNFT by a factor more than 50. The exceptions to this pattern are metal fumes and combustion aerosols where the small particle size distributions result in QNFT fit factors that are larger than predicted workplace protection factor by a factor of as much as 2.4. This situation could cause a potential overexposure, especially when the QNFT test is used as the basis for assigning a protection factor greater than the customary one, a procedure provided for in ANSI Z88.2-1980.⁽¹²⁾

At higher QNFT fit factors, leakage is less, so overall performance is controlled to a greater extent by filter penetration rather than facial-seal leakage. Consequently, for small particle sizes where filter penetration is greatest, the predicted protection factors are lower relative to the corresponding QNFT fit factors.

A separate analysis was conducted using the model to isolate the effects due to the different variables for the first row of Table I. The difference in work rate (0 kg-m/min for test, 415 kg-m/min for use) increases the protection factor by 30 percent. The difference between the test and use filters decreases the protection factor by 21 percent. The difference between the test and use aerosol size distribution causes a 53 percent increase in protection factor. The small remaining difference is due to the difference between the average percent leakage for the range

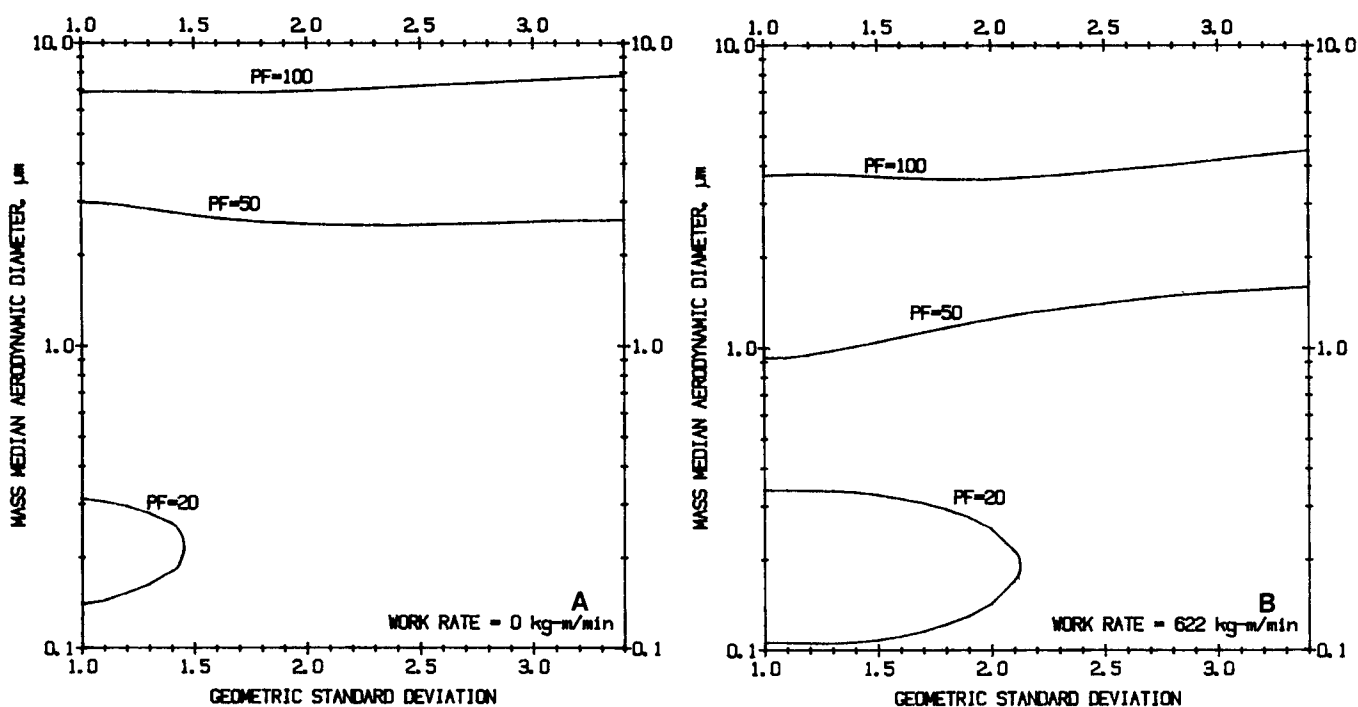


FIGURE 1. Predicted protection factor contours for dust, fume, and mist half-mask respirator having a 2% facial-seal leak at a total flow of 34.3 lpm; a) work rate equals 0 kg-m/min; b) work rate equals 622 kg-m/min.

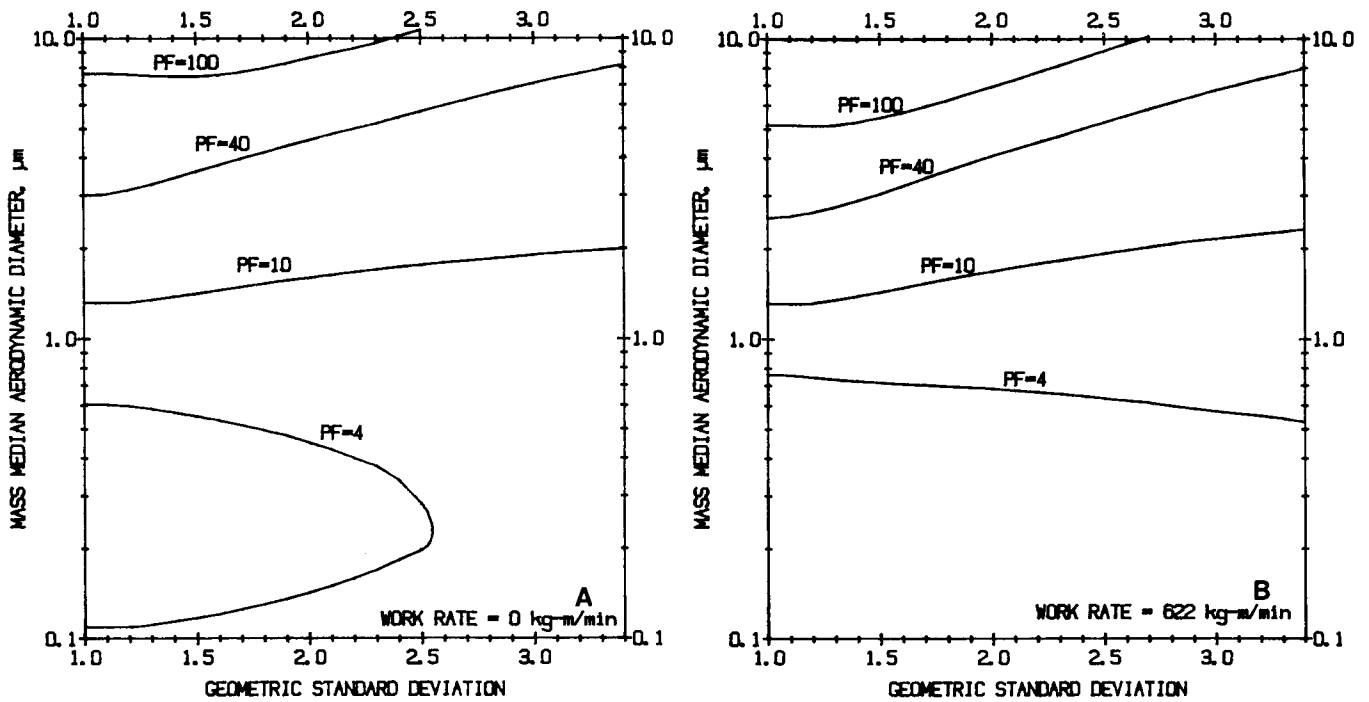


FIGURE 2. Predicted protection factor contours for disposable dust and mist respirators having a 2% facial-seal leak at a total flow 34.3 lpm; a) work rate equals 0 kg-m/min; b) work rate equals 622 kg-m/min.

of flow rates associated with a work rate of 0 kg-m/min and the percent leakage at the average flow rate for 0 kg-m/min, 34.3 lpm.

The information given above can be put in a more general form as shown in Figures 1a and 1b. These graphs assume the exposure aerosol size distribution is lognormal and show contour lines of predicted protection factor for different values of MMAD and GSD. The graph thus allows estimation of a workplace protection factor for a respirator with a specified facial-seal leak and a lognormal exposure aerosol size distribution having a MMAD and GSD within the limits of the graph. A GSD of 1.0 corresponds

to a monodisperse aerosol (all particles the same size), and a GSD of 3.5 corresponds to an aerosol with a wide size distribution.

Figure 1a is for the case of an average DFM half-mask respirator with a 2 percent leak at 34.3 lpm and a work rate of 0 kg-m/min. Figure 1b is the same except the work rate is 622 kg-m/min. A 2 percent leak at 34.3 lpm means that at this flow rate, 2 percent of the air flow goes through the facial-seal leak and 98 percent through the filters. Figures 2a and 2b show similar information for disposable respirators (average of three

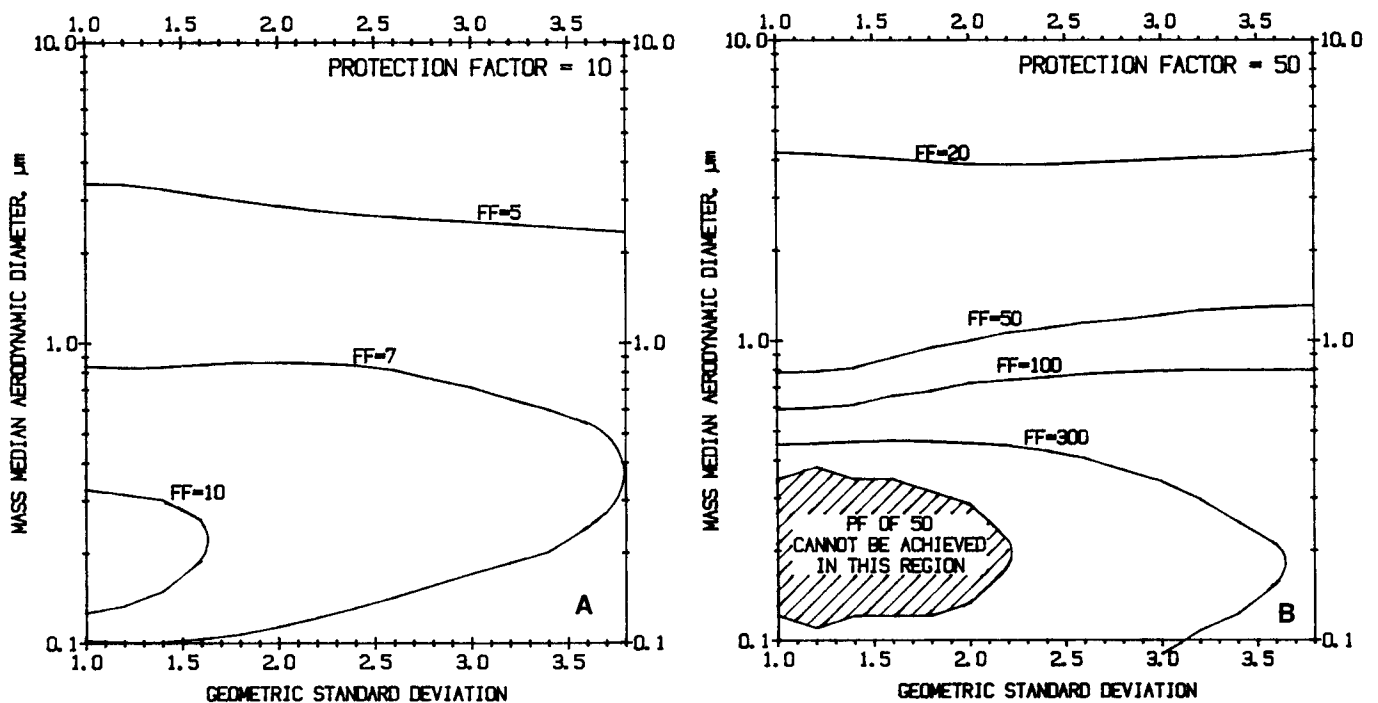


FIGURE 3. a) QNFT fit factor required to achieve a protection factor of 10 at a work rate of 415 kg-m/min; b) QNFT fit factor required to achieve a protection factor of 50 at a work rate of 415 kg-m/min.

brands with dust and mist approval) with the same 2 percent leak at 34.3 lpm.

In both Figures 1 and 2, there is evidence of improved overall performance as MMAD decreases below 0.2 μm . This effect is a result of improved filter performance due to particle capture by diffusion for particles less than 0.2 μm . The results in Figure 1 cannot be compared directly with Table I. Figure 1 is for a respirator with a 2 percent leak and a DFM filter, whereas predicted protection factors in Table I are for a respirator having the indicated fit factor as measured by QNFT with DFMR filters at 0 kg-m/min, but used at 415 kg-m/min with DFM filters. Unfortunately, one needs a whole set of graphs, like Figure 1, covering many different leakage rates (or QNFT measurements) and work rates to predict actual use performance and worker exposure. The model described in reference 2 could be used to construct such a set of graphs.

The information presented in Figures 1 and 2 can be presented in a different way as shown in Figures 3a and 3b. The contour lines in these figures represent the QNFT fit factor required to achieve an overall protection factor of 10 and 50 at a 415 kg-m/min work rate for a given MMAD and GSD. The use of Figures 1 and 2 requires one to assume that the fit measured during QNFT is representative of the fit achieved in use. For large particle sizes (MMAD), fit is less important for achieving a given overall protection factor than it is for submicrometer sizes. For most submicrometer particle size distributions, a QNFT fit factor greater than 100 is required to achieve an overall protection factor of 50, Figure 3b. For size distribution in the shaded region of Figure 3b, an overall protection factor of 50 is not possible because particle penetration through the average DFM filters represents more than 2 percent of exposure aerosol concentration.

The analysis given above accepts the QNFT as being an accurate evaluation of fit and does not consider, for example, how data are averaged for the different exercises. Figures 1 and 2 predict only respirator performance while the mask is being worn properly and having the specified 2 percent leak at 34.3 lpm. Figure 3 predicts only the QNFT fit factor required to achieve the indicated level of overall protection when the mask is worn properly by a worker working at a work rate of 415 kg-m/min.

Conclusions and Recommendations

Applications of a previously reported computer model for predicting the performance of half-mask respirators for protection against aerosols based on quantitative fit test results, the type of respirator filter used, and exposure conditions of work rate and aerosol size distribution are presented for a wide range of industrial exposure conditions. Based on published size distributions, properly conducted QNFT measurements using current equipment accurately reflect facial-seal leakage with the particle size dependent loss in facial-seal leaks introducing an error of less than 5 percent. Based on the particle size limits recommended in Z88.2-1980,⁽¹²⁾ instruments relying on forward light scattering particle detection may underestimate leak penetration by up to 23 percent.

For normal working conditions, a work rate of 0 to 622 kg-m/min, persons wearing a half-mask cartridge respirator, with DFM filters having average performance, need to have a measured QNFT fit factor of 15 or greater in order to be sure of achieving an overall protection factor of 10 in use. This assumes that the QNFT test is conducted at a work rate of 0 kg-m/min with DFMR filters having zero penetration and average resistance

and that the fit measured during QNFT is representative of the fit achieved in use. For workers exposed to aerosols with MMADs greater than 1.0 μm , a fit factor of 11 is required to achieve an overall protection factor of 10 in use. To achieve an overall protection factor of 50 with DFM filters for exposure aerosols having MMADs greater 1.0 μm , the QNFT fit factor must be greater than 85.

Because of the difficulties of making and interpreting QNFT measurements with disposable dust and mist respirators, similar fit factor recommendations can not be made. Based on Figures 2a and 2b, one can estimate that a facial-seal leakage of less than 2 percent is required to achieve an overall protection factor of 5 for the average disposable dust and mist respirator if the exposure particle size distribution has a MMAD greater than 1.0 μm . This would be equivalent to a QNFT fit factor of 50 determined for a test respirator having zero filter penetration of the test aerosol and the same resistance as the dust and mist disposable respirator.

Acknowledgment

This research was supported in part by PHS (NIOSH) Grant Number 1R01 OH01595.

References

1. Hinds, W.C.; Kraske, G.: Performance of Dust Respirators with Facial-seal Leaks: I. Experimental. *Am. Ind. Hyg. Assoc. J.* 48:836 (1987).
2. Hinds, W.C.; Bellin, P.: Performance of Dust Respirators with Facial-seal Leaks: II. Predictive Model. *Am. Ind. Hyg. Assoc. J.* 48:842 (1987).
3. Silverman, L.; Plotkin, T.; Sawyers, L.A.; Yancey, A.: Air Flow Measurements on Human Subjects With and Without Respiratory Resistance at Several Work Rates. *Arch. Ind. Hyg. Occup. Med.* 3:461 (1951).
4. Silver, L.; Davidson, G.; Jansson, D.; et al: Analytical Modeling of Respiratory Protective Devices. *Am. Ind. Hyg. Assoc. J.* 32:775 (1971).
5. Campbell, D.L.: The Theoretical Effect of Filter Resistance and Filter Penetration on Respirator Protection Factors. *J. Int. Soc. Resp. Prot.* 2:198 (1984).
6. Williams, F.T.: An Analytical Method for Respirator Performance Prediction Utilizing the Quantitative Fit Test. *J. Int. Soc. Resp. Prot.* 1:109 (1983).
7. Lowry, P.L.; Revoir, W.H.: Comparison of a Sodium Chloride Aerosol Filter Test Method to Silica-dust and Silica-mist Filter Test Methods. *Am. Ind. Hyg. Assoc. J.* 39:709 (1978).
8. Product information, "TDA-60 NaCl aerosol man test system." ATI, Baltimore, MD 21207.
9. Product information, "Model 264/223 portable respirator fit test system." Dynatech Frontier Corporation, Albuquerque, NM 87110.
10. Hinds, W.C.; Macher, J.M.; First, M.W.: Size Distribution of Aerosols Produced by the Laskin Aerosol Generator Using Substitute Materials for DOP. *Am. Ind. Hyg. Assoc. J.* 44:495 (1983).
11. Dave, J.V.: Subroutines for computing the parameters of electromagnetic radiation scattered by a sphere. Report No 320-3237. IBM Scientific Center, Palo Alto, CA (1968).
12. American National Standard Practices for Respiratory Protection, Z88.2-1980. American National Standards Institute, New York (1980).
13. Taylor, C.D.; Jankowski, R.A.; Ruggieri, S.K.; Muldoon, T.L.: Use of Instantaneous Samplers to Evaluate the Effectiveness of Respirable Dust Control Methods in Underground Mines. In: *Aerosols in the Mining and Industrial Work Environments*, pp. 447-449. V.A. Marple and B.Y.A. Liu, Eds. Ann Arbor Science, Ann Arbor, MI (1983).
14. Tomb, T.F.; Treafits, H.N.; Gero, A.J.: Characteristics of Underground Coal Mine Dust Aerosols. *Ibid.*, pp. 399-403.
15. Treafits, H.N.; Kacsmar, P.; Suppers, K.; Tomb, T.F.: Comparison of Particle Size Distribution Data Obtained with Cascade Impaction Samples and from Coulter Counter Analysis of Total Dust Samples. *Am. Ind. Hyg. Assoc. J.* 47:87 (1988).
16. Burkhart, J.E.; McCawley, M.A.; Wheeler, R.W.: Particle Size Distribu-

- tions in Underground Coal Mines. Presented at the American Industrial Hygiene Association Conference, Philadelphia, PA (1983).
17. Hargis, K.M.; Tillery, M.I.; Gonzales, M.; Garcia, L.L.: Aerosol Sampling and Characterization in the Developing U.S. Oil Shale Industry. In: *Aerosols in the Mining and Industrial Work Environments*, pp. 491–496. V.A. Marple and B.Y.A. Liu, Eds. Ann Arbor Science, Ann Arbor, MI (1983).
 18. Froines, J.R.; Liu, W.-C.V.; Hinds, W.C.; Wegman, D.: Effect of Aerosol Size on the Blood Lead Distribution of Industrial Workers. *Am. J. Ind. Med.* 9:227 (1986).
 19. Drinker, P.; Hatch, T.: *Industrial Dust: Hygienic Significance, Measurement and Control*, pp. 220–224. McGraw-Hill Book Company, New York (1936).
 20. Bamford, W.D.: *Control of Airborne Dust*, p. 226. The British Cast Iron Research Association, Alvechurch, Birmingham, England (1961).
 21. Cohen, B.S.; Harley, N.H.; Martinelli, C.A.; Lippmann, M.: Sampling Artifacts in the Breathing Zone. In: *Aerosols in the Mining and Industrial Work Environments*, pp. 350–351. V.A. Marple and B.Y.A. Liu, Eds. Ann Arbor Science, Ann Arbor, MI (1983).
 22. Hoover, M.D.; Newton, G.J.; Yeh, H.C.; Edison, A.F.: Characterization of Aerosols from Industrial Fabrication of Mixed-Oxide Nuclear Reactor Fuels. *Ibid.*, p. 541.
 23. Droz, P.: Personal communication (1987).
 24. Wesley, R.A.; Hatcher, J.D.; McCaskill, O.L.; Cocke, J.B.: Dust Levels and Particle-Size Distributions in High-Capacity Cotton Gins. *Am. Ind. Hyg. Assoc. J.* 39: 368 (1978).
 25. Cinkotai, F.F.: The Size-distribution and Protease Content of Airborne Particles in Textile Mill Cardrooms. *Am. Ind. Hyg. Assoc. J.* 37:234 (1976).
 26. Donham, K.J.; Scallon, L.J.; Poppendorf, W.; et al: Characterization of Dusts Collected from Swine Confinement Buildings. *Am. Ind. Hyg. Assoc. J.* 47:404 (1986).
 27. Darcy, F.J.: Physical Characteristics of Wood Dusts, pp. 91–93. University of Minnesota Ph.D. Thesis 1982. University Microfilms International, Ann Arbor, MI.
 28. McCammon, Jr., C.S.; Robinson, C.; Waxweiler, R.J.; Roscoe, R.: Industrial Hygiene Characterization of Automotive Wood Model Shops. *Am. Ind. Hyg. Assoc. J.* 46:343 (1985).
 29. Hewitt, P.J.; Hicks, R.; Lum, H.F.: The Generation and Characterization of Welding Fumes for Toxicological Investigations. *Ann. Occ. Hyg.* 21:159 (1978).
 30. Japuntich, D.A.; Johnson, B.D.: Characteristics of Lead Fume Aerosol Generated Under Different Conditions by an Oxygen-Natural Gas Welding Torch. In: *Aerosols in the Mining and Industrial Work Environments*, p. 517. V.A. Marple and B.Y.A. Liu, Eds. Ann Arbor Science, Ann Arbor, MI (1983).
 31. Casey, P.; Haggen, R.; Harper, P.: A Collaborative Study of 'Ink Mist' in U.K. Newspaper Press Rooms. *Ann. Occ. Hyg.* 27:127 (1983).
 32. Ackley, M.W.: Paint Spray Tests for Respirators: Aerosol Characteristics. *Am. Ind. Hyg. Assoc. J.* 41:309 (1980).
 33. Mokler, B.V.; Damon, E.G.; Henderson, T.R.; Jones, R.K.: Consumer Product Aerosols: Generation, Characterization and Exposure Problems. In: *Generation of Aerosols and Facilities for Exposure Experiments*, pp. 584–5. K. Willeke, Ed. Ann Arbor Science, Ann Arbor, MI (1980).
 34. Goldsmith, A.H.; Vorpahl, K.W.; French, K.A.: Health Hazards from Oil, Soot and Metals at a Hot Forging Operation. *Am. Ind. Hyg. Assoc. J.* 37:217 (1976).
 35. Futagaki, S.K.: Petroleum Refinery Workers Exposure to PAHs at Fluid Catalytic Cracker, Coke and Asphalt Processing Units. U.S. Dept. of Health and Human Services, NIOSH Contract No 210-78-0082. Cincinnati, OH (1983).
 36. Hinds, W.C.: Size Characteristics of Cigarette Smoke. *Am. Ind. Hyg. Assoc. J.* 39:48 (1978).
 37. Muskett, C.J.; Caswell, R.: An Investigation Into Lead in Two Indoor Small-Bore Rifle Ranges. *Ann. Occ. Hyg.* 23:283 (1980).
 38. Kittelson, D.B.; Dolan, D.F.: Diesel Exhaust Aerosols. In: *Aerosols in the Mining and Industrial Work Environments*, pp. 339–343. V.A. Marple and B.Y.A. Liu, Eds. Ann Arbor Science, Ann Arbor, MI (1983).

Received 2/18/87; review/decision 4/13/87; revision 12/2/87; accepted 12/14/87